TORSIONAL LOW CYCLE FATIGUE OF DIFFERENT STEELS

G. KOMPEK, K.L. MAURER*

Crack initiation and crack propagation were studied in twist-controlled torsional low cycle fatigue tests. At the two low carbon steels investigated fatigue bands were formed in the two directions of maximum shear stresses in the first fatigue stage. First microcracks appear at these bands later on. In contrast to this, nonmetallic inclusions were nucleation sites for the crack initiation in the quenched and tempered steel. A comparison of the three steels investigated showed that crack propagation rate was highest in the quenched and tempered steel, whereas it was slowest in the low carbon steel with 0,12% C. There was no difference in the fracture mode between crack initiation and propagation.

INTRODUCTION

In recent studies in the field of fatigue of materials the push-pull-loading (Mode I) has dominated almost exclusively. Investigations about the torsional fatigue behaviour (Mode III), however, hardly exist. Only in the last 5 years a few studies were published dealing with torsional fatigue, primarily dealing with the crack propagation behaviour (1-5). Investigating a quenched and tempered steel Ritchie et al. (7) developed a micromechanical model for fatigue crack propagation at Mode III loading. According to this model fatigue crack initiation and propagation take place in Mode I at low shear stresses ($\tau/\tau_S<0,7$) and at higher shear stresses ($\tau/\tau_S>0,85$) in a combined Mode III + II; the crack in Mode II starts at inclusions ahead of the crack tip.
Comparing investigations of Mode III with Mode I crack propagation, comparable loading conditions at Mode III rates are 10 to 50 times slower than at Mode I (3,6). Tschegg (7) explained this by fracture surfaces in sliding contact. Therefore the applied load is reduced to a smaller effective load ΔK_{IIIeff} at the crack tip. After elimination of these rubbing influences by extrapolation to a crack length of c=0 a so called "true" Mode III-crack propagation curve can be obtained lying over the Mode I-curve (7). Explanations of the varying behaviour of cracks at crack initiation and propagation in regard to the microstructure are very incomplete. Therefore here the phenomena of crack initiation and propagation depending on load and microstructure were investigated at three different steels.

* Institut für Metallkunde und Werkstoffprüfung
Montanuniversität Leoben, Austria

MATERIAL AND EXPERIMENTAL PROCEDURE

Fatigue tests were performed in twist control (R=-1) at a Schenck-torsion fatigue testing machine on smooth and notched cylindrical specimens. By an elastic movable grip in longitudional direction tensile stresses were eliminated. Investigations for crack initiation were performed mainly on smooth samples (diameter of 15 mm) and investigations for crack propagation on circumferentially notched samples (notch depth 1 mm, angle 90°, notch radius ≈0,05 mm).

Table 1: Composition of the steels

Steel No.	Element (wt.%)										
	C	Si	Mn	Cr	Ni	Mo	Cu	V	Al	P	S
1(C 2)+	0,02	0,13	0,36	-	0,04	-	0,03	-	0,008	0,022	0,017
2(C 12)+	0,12	0,17	0,37	0,01	0,02	-	0,01	0,01	0,030	0,022	0,016
3(34CrNiMo6)*	0,32	0,32	0,43	1,43	1,46	0,16	0,18	-	-	0,020	0,024

+ normalized at 950°C
* austenitized at 930°C, oil quenched, tempered at 650°C

The chemical compositions of the three steels selected for this study are given in Table 1. No 1 and 2 are low carbon steels with different carbon contents, whereas No 3 is a quenched and tempered steel. Both low carbon steels were normalized at 950°C for half an hour followed by furnace cooling obtaining a ferritic and a ferritic-pearlitic microstructure. The heat-treated steel was austenitized at 930°C for half an hour followed by oil quenching and tempering at 650°C for an hour and a quarter obtaining tempered martensite. The mechanical properties of these steels are summarized in Table 2.

Table 2: Mechanical properties of the steels

Mechanical Properties			Steel No.		
			1	2	3
Tensile yield (proof) strength	R_{eH}, $R_{p0,2}$	[MPa]	215	199	870
Tensile strength	R_m	[MPa]	317	373	970
Elongation	A_5	[%]	45	22	16
Reduction of area	Z	[%]	74	66	67
Mean intercept length of ferrite grains	$\bar{L}$	[µm]	63	41	--

After distinct numbers of cycles the crack grwoth was determined by the heat-tinting method. This enables an easier distinction between fatigue and final fracture (in liquid nitrogen) to determine the different crack lengths. Because of rubbing fracture surfaces, which is a statistical process, the D.C.electric potential technique cannot be used for crack length measurement. To omit possible errors, correct crack length measurements are

only possible at an applied axial load so that an influence of Mode I has to be expected. Determinations of da/dN-ΔKIII-curves are difficult due to irregular crack fronts and numerous branches of cracks in two almost equivalent shear systems. The plastic zone is often so large that the validity of the fracture-mechanics is not given.

RESULTS

The investigations are confined to low cycles fatigue. The low cycle fatigue behaviour is described by the Manson-Coffin law. Generally fatigue cracks nucleate at areas with high slip concentrations. If the permanent irreversible plastic deformations exceed a distinct critical value, microcracks appear.

Crack initiation

Comparing the low carbon steels with the quenched and tempered steel different surface morphology until the first microcracks appear is observable. At steels 1 and 2 fatigue bands were formed, shown in Fig.1a for steel 1 and in Fig.1b for steel 2. Those fatigue bands are normally orientated along the two directions of maximum shear stresses, which are the directions parallel and perpendicular to the torque axis at torsional loading (8). This was valid for all loading conditions in high and low cycle fatigue. Firstly fatigue bands were formed within grains on slip planes favourably orientated in the directions of the two maximum shear stresses.After further cycles in the other surface grains slipping occured.Many of the less ideally oriented crystals turn to a more suitable position to both directions of maximum shear stresses and a typical texture arises at the surface (9).
In those fatigue bands very distinct extrusions can often be seen (Fig. 1).These first growing microcracks join together to a crack network at the surface of steel 1. Longitudinal cracks were created at steel 2 rather than at steel 1 (this is caused by the longitudinal orientation of the pearlite colonies in the samples). Microcracks were also formed in samples, loaded in the fatigue strength region, but these microcracks were not able to grow (see Fig.2). Nonmetallic inclusions had no influence on the crack initiation. They only decohered from the matrix during the fatigue process. They were obviously not so effective as stress raisers. In the ferritic-pearlitic steel (steel 2) pearlite did not take part in the deformation process at the surface. In most cases the cracks stop at the pearlite-ferrit boundaries or branch (see Fig.1b). Fig.3 shows a transverse micro-section of a fatigued specimen,where toothed grain boundaries indicate slip processes within grains below the surface. The cracks grow extensively in a transcrystalline manner and the few precipipated cementite plates at the grain boundaries have no influence on the crack growth behaviour. Strain hardening and softening processes investigated at this stage in dependence of the cyclic loading amplitude will be discussed in another paper (10).

Contrary to the low carbon steels the quenched and tempered steel had a different behaviour at the beginning of the cycling. Obviously the nonmetallic inclusions in this steel have a strong influence as stress raisers (see Fig.4). First, nonmetallic inclusions decohere from the matrix often pro-

ducing cracks being able to grow.

Crack propagation

The three steels investigated show distinct differences in the crack growth behaviour. In order to get comparable conditions, the plastic shear strain amplitude has been kept constant over the whole range of investigated crack propagation. Due to the notch the whole strain is being localized in the notch area and the plastic shear strain range $\Delta\gamma_{pl}$ estimated for this area was $\Delta\gamma_{pl} \approx 4{,}5\%$. Fig.5 shows that cracks in the quenched and tempered steel are growing faster than in the two low carbon steels. Especially steel 2 with the higher pearlite content shows a significant retardation of crack growth after crack propagation of about 0,8 mm. Typical macroscopic fractographs are shown in Fig.6. The dark area represents the oxydized fatigue crack surface marked by the heat-tinting method and the light area the final impact fracture at liquid nitrogen temperature. In all cases a more or less extended concentric rim of a flat fracture mode appeared. The extension of the rim zone at the same number of cycles depends on the strain amplitude, the mechanical properties of the material and the microstructure. There is no change in the macroscopic fracture appearance till the final fracture in the low carbon steel 1 occurs (Fig.7). The whole fracture surface shows rubbing marks on the horizontal parts of the steps. No typical striations of fatigue, known from Mode I tensile load are visible. This appearance is nearly the same at all applied plastic shear strain amplitudes over the whole fracture surfaces.

There are only few differences of the fracture surface appearance of steel 1 and 2 at the same loading conditions at the beginning of crack propagation. The scanning micrograph (Fig.8) shows somewhat higher steps compared to Fig.7. The surface is destroyed by heavy rubbing marks as in the low carbon steel 1. Only at very few areas lying on lower planes faint traces of striations are visible similar to the generally known pattern produced in Mode I load. The distances of these striations (about 1 µm) are comparable to the crack propagation rate but it is not evidence enough to associate these striations with Mode III + II propagation. In the case of an inclination of the crack surface Mode I crack propagation is possible here. After a certain number of cycles depending on the applied amplitude the fracture surface becomes lamellar like blockies (Fig.8). This appearance is also shown in the macrograph (Fig.6b). Cracks are running radial and tangential lying nearly normal to the crack surface subdividing the structure in geometrical components. This blocky structure becomes larger the further the crack propagation proceedes. After heat-tinting and final impact fracture in liquid nitrogen this steel shows cracks normal to the crack front running on in front of the proper crack front into the final cleavage fracture (Fig.9). These cracks are not caused by the impact because they exhibit the dark colour of the heat tinting procedure. A micrograph of a cross section normal to these cracks shows below the electrolytical Ni deposit the geometrical blocky structure (Fig. 10). The cracks are lying in the ferrite parallel to the rolling texture and normal to the main crack front. Very often transverse cracks subdivide the cracked lamellas into seperated components. The whole structure looks desintegrated.

In the quenched and tempered steel 3 the fracture surface looked similar to that of low carbon steels. Macroscopically it was more flat and there were radial cracks to a lower extent. In other tests (in steel 3), where the shear strain amplitude was not kept constant, a change of a firstly macroscopic flat fracture surface to the so called factory roofs appeared after some crack propagation (Fig.11). There is some evidence that this is connected with a change of the crack propagation Mode III + II to the Mode I (4). The factory roof surfaces are located normal to the maximum tensile stress (about 45° to the main crack). Fig.11 shows the scanning micrograph with radial river pattern in the inclined plane marking the direction of crack propagation. Striations typical for Mode I crack propagation in materials with a sufficient plasticity are not detectable. The higher the starting plastic shear strain amplitude was, the later the factory roofs were formed.

DISCUSSION

The plastic strains by fatigue loading form cracks after a certain number of cycles depending on different materials. In all cases the formation of cracks starts at the surface if there are no stress raisers beyond the surface.
Crack initiation is additionally promoted if the highest stresses appear at the surface like in torsional load investigated in this paper. Surface crystals deform more easily than the crystals situated below due to the plane state of stress, so that the gliding per cycle is greater in the surface crystals and the necessary number of cycles for the crack initiation is smaller at the surface than inside. A progress in fatigue loading results in a roughening of the surface (11).

It depends on the strength of steels whether nonmetallic inclusions influence the crack initiation. Contrary to Tipnis and Cook (12), who found an influence of inclusions in all their investigations, we were only able to determine a clear influence at the surface of the quenched and tempered steel.
The first microcracks are orientated in both directions of maximum shear stresses. At low stresses ($\tau/\tau_S < 0{,}7$) Ritchie et al (3) also found crack initiation in Mode I at notched specimens from AISI 4340 steel fatigued in torsion. Normally in smooth specimens the cracks in high strength steels will be only initiated as tensile stress cracks inclined about 45° to the specimen axis, if the ultimate tensile strength exceeds $R_m > 1100\ N/mm^2$. Furthermore the crack initiation in smooth specimens is irregularly distributed over the circumference at the surface of the specimens. Only some of these cracks will be able to grow and the consequence of the inward and outward crack propagation will be an irregularly shaped crack with steps. If the cracks are created as shear cracks in the maximum shear directions or as cracks normal to the maximum tensile stress in the specimen, there is no fundamental difference in the mode between crack initiation and crack propagation by alternating torsional loading. Initiation and propagation mode essentially depends on the flow stress, the ultimate tensile strength of the material and secondly on the load conditions and the microstructure. The cracks join together after a distinct distance of propagation on the crack plane.

In the case of low carbon steels the cracks start at the

surface in the two perpendicular shear directions indicating the blocky fracture surface. In specimens with a circumferential notch, crack initiation is caused by the stress intensity of the notch and is therefore restricted to the small area at the notch tip with the maximum strain. The stress concentration due to the notch causes propagation of only one crack perpendicular to the torque axis is different to smooth specimens. Propagation of fatigue cracks was now governed essentially by deformation processes in the plastic zones in front of the crack tip. The more the influence of the stress field of the notch diminishes the more the deformation in the plastic zone will be active. In high strength steels small alternating stress intensity factors ΔK result in small plastic zones being responsible for a factory roof appearance due to crack propagation normal to the tensile stress. There are not so many cracks visible normal to the crack surface in the area with crack advance in Mode III + II and at the crack surface created by Mode I as well, thus indicating the reduced possibility of shear in this material and at this stress condition. Higher amplitudes result in larger plastic zones and more possibilities of shear mechanisms. Crack advance in Mode III and II can occur more easily. After leaving the stress influenced area of the notch growing cracks can advance mutually at right angles in the two main shear directions in the two low carbon steels. Beside the topography effect of the main crack surface the dissipated crack energy and strain energy of the crack tips in several crack systems might be a further reason for the reduction of crack propagation rate in comparison to the quenched and tempered steel.

Obviously in the low carbon steel 2 the main crack propagation occurs favourably normal to the specimen axis in Mode III and II. Tschegg (13) suggested that in low carbon steels with a ferrite-pearlite structure a superimposed static load Mode I to the alternating torsion is responsible for a lamellar fracture appearance on the crack surface. There is some evidence now that in low carbon steels with a ferrite-pearlite structure the rolling texture causes an extensive crack growth in shear directions lying perpendicular to the shear direction of the main crack. Different cross sections parallel to the specimen axis clearly showed the desintegration of the structure like bonds in a small masonry (Fig. 10). The size of the blockies in the cross directions corresponds to the distance of the pearlite rows. Cross sections in front of the crack front display fatigue cracks running on in front of the main crack front and lying perpendicular to the main crack. Apparently the pearlite lines act as obstacles for gliding motions in order to prevent a privilege fatigue crack propagation in the shear directions perpendicular to the specimen axis. This suggestion is even more evident, because in smooth specimens with ferrite-pearlite lines crack initiation and propagation arise preferable parallel to the specimen axis.

Propagation of fatigue cracks was governed essentially by deformation processes in the plastic zones in front of the crack tips. Difficulties arise at investigations of crack growth rates by alternating torsional loading. All attempts go gain a true da/dN-ΔK_{III}-dependence did not work, because it is nearly impossible to eliminate the influence of the rubbing surface,without changing the mode characteristics (6). Attempts of Tschegg (13), who took the relatively large plastic zone with

the plastic strain intensity concept into account, give a first information about the crack growth behaviour. By extrapolation of the crack propagation rate to a crack length of c=0, he was able to get the crack growth rate without the influence of the rubbing crack surface. In our investigations the size of plastic zones is very large, especially in the low strength low carbon steels. A method for estimating the true size of the plastic zone by torsional loading very roughly is the recrystallisation method (14,15). But this method does not work in materials with more than one phase (ferrite-pearlite and quenched and tempered structures). Furthermore it would be necessary to consider work softening and work hardening in the plastic zone. In consequence of this uncertainties we restricted our investigations of crack growth keeping the plastic shear strain range constant. The size of the plastic zone should be more or less constant during crack propagation. The effective ΔK_{III} becomes smaller during crack propagation according to the increase of friction and the cracks can be stopped. Fig.5 shows that as long as no factory roofs appear on the fracture surface of the quenched and tempered steel the crack propagation rate is highest due to a relatively smooth crack surface. The quantity of radial cracks in the perpendicular shear system is not as high as in the low carbon steels. The break in the curve of the steel with ferrite-pearlite structure is due to the increasing blocky surface structure. Therefore the main difference in crack propagation rate can only be seen in regard to the whole topography of the crack surface.

CONCLUSION

Crack initiation and crack propagation have been studied at two low carbon steels (with 0,02 and 0,12% carbon) and at one quenched and tempered steel (34CrNiMo6) in twist-controlled torsional low cycle fatigue tests.
In the first fatigue stage the two low carbon steels form fatigue bands in the two directions of maximum shear stresses. First microcracks were created at this bands. In contrast to these steels nonmetallic inclusions at the quenched and tempered steel have an effect on crack initiation as stress concentrators. A comparison of the three steels investigated shows that the crack propagation rate was highest in the quenched and tempered steel whereas it was lowest in the low carbon steel with 0,12% carbon..

In smooth specimens there is no difference in the fracture mode between fatigue crack initiation and propagation. Firstly depending on the strength of materials cracks nucleate and grow in shear bands (Mode III + II) or in a tensile mode (Mode I). Plastic strain amplitude and microstructure can influence the crack behaviour. For instance in high strength steels a small plastic zone favours a tensile crack Mode I. In low carbon steels pearlite rows favour shear band crack initiation and propagation parallel to the rows. In circumferential notched specimens the stress field of the notch influences the crack initiation and the first crack propagation. The further crack advance followed the same principles as in the smooth specimens. The crack propagation rate is mainly influenced by the topography and energy dissipating processes on the rubbing crack surfaces.

ACKNOWLEDGEMENT

The Fonds zur Förderung der Wissenschaftlichen Forschung in Österreich is greatfully acknowledged for sponsering this investigation. The authors thank G. Schindelbacher and H. Strohmeier for helping at diverse experimental works.

REFERENCES

1. Pook, L.P., and Sharples, J.K., 1979, Int.J.Frac.,15, R223

2. Hurd, N.J., and Irving, P.E., 1982, ASTM STP 761, 212

3. Ritchie, R.O., McClintock, F.A., Hashemi,H.N., and Ritter, M.A., 1981, Metall.Trans.A, 13A, 101

4. Tschegg, E.K., 1982, Mater.Sci.Eng., 54, 127

5. Kompek, G., Matzer, F.E., and Maurer, K.L., 1982, Proc. ECF4, Leoben, 398

6. Hurd, N.J., and Irving, P.E., 1980, Proc.3.Colloqu.on Fracture, London, 239

7. Tschegg, E.K., 1982, J.Mater.Sci., 18, 1604

8. Dieter, G.E., 1961,"Mechanical Metallurgy",McGraw-Hill Book Company, New York, 273

9. Regenet, P.J., and Stüwe, H.P., 1963, Zeitschr.f.Metallk., 54, 273

10. Kompek, G., and Maurer, K.L., 1984, Proc.Fatigue 84, Birmingham, in press

11. Munz, D., Schwalbe K., and Mayr, P., 1971, "Dauerschwingverhalten metallischer Werkstoffe", Vieweg, 90

12. Tipnis, V.A., and Cook, N.H., 1967, I.Basic Eng., Trans. ASME Ser.D, 89, 533

13. Tschegg, E.K., 1983, Mat.Sci.Eng., 59, 127

14. Mitsche, R., Stanzl, S., and Matzer, F., 1974, Arch. Eisenhüttenwesen, 45, 179

15. Kompek, G., Matzer, F., and Maurer, K.L., 1983, Sonderb. Prakt. Metallogr., 10, 497

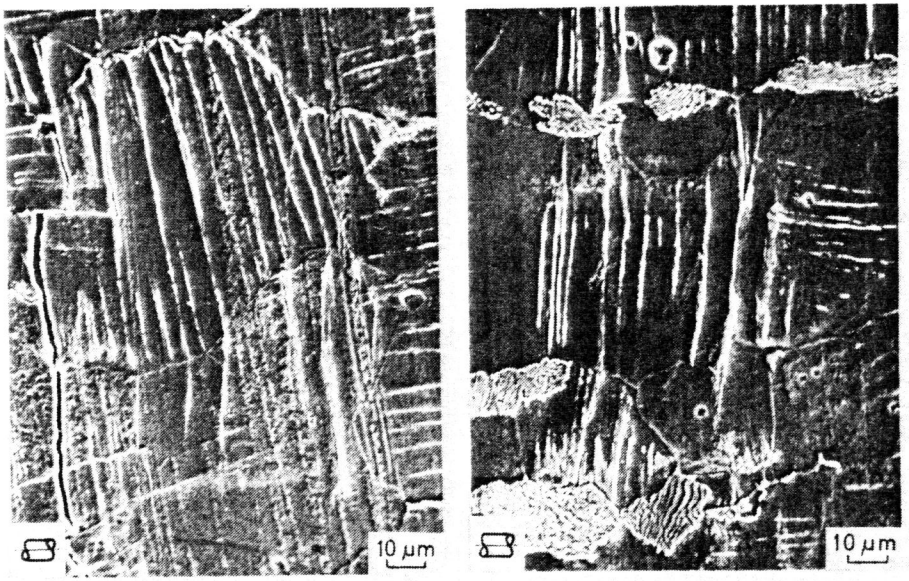

Fig.1 Fatigue bands with extrusions and microcracks in low carbon steels
a) Steel 1 (0,02 % carbon) b) Steel 2 (0,12 % carbon)

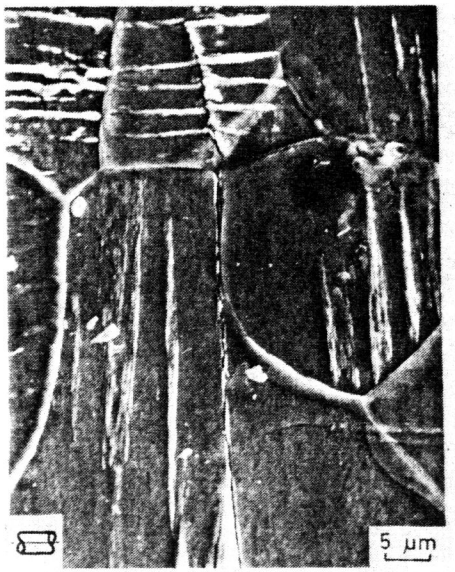

Fig.2 Fatigue bands and microcracks in steel 2 tested below the fatigue limit

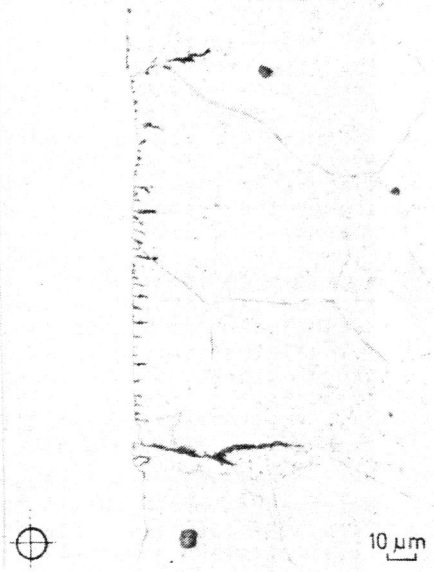

Fig.3 Transverse micro-section of a fatigued specimen (steel 1; the surface is nickel-plated)

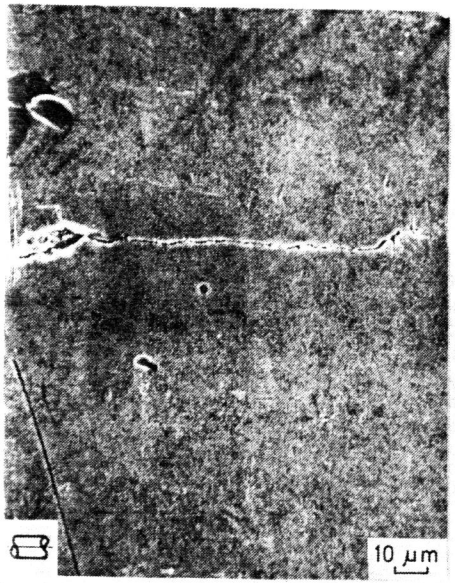

Fig.4 Crack initiation at non-metallic inclusions in quenched and tempered steel

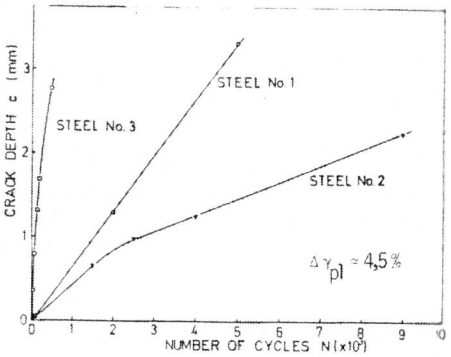

Fig.5 Crack propagation at constant cyclic plastic strain amplitude ($\Delta\varphi_{pl}=0,59° \rightarrow \Delta\gamma_{pl}=4,5\%$)

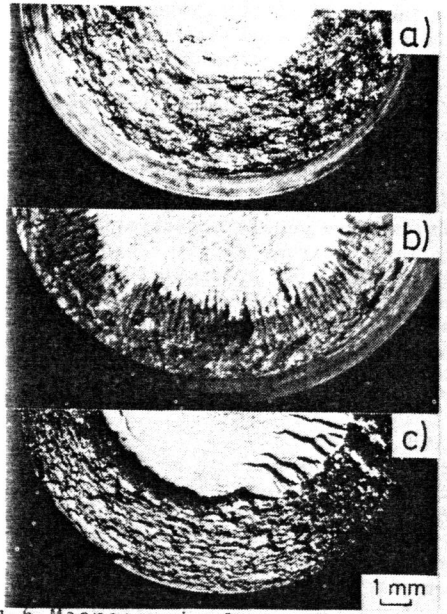

Fig.6 Macroscopic fracture surfaces (final fracture in liquid nitrogen)
a) Steel 1 b) Steel 2
c) Steel 3

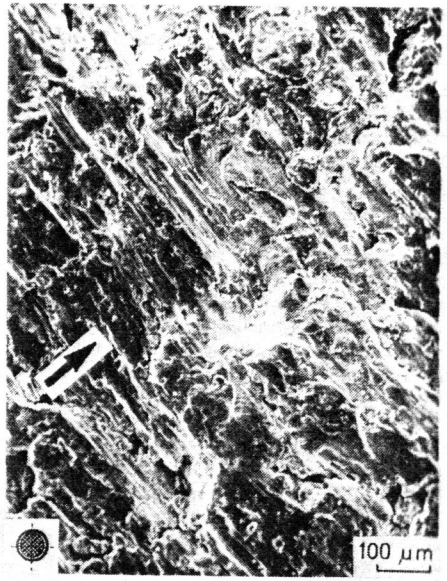

Fig. 7 Rubbing marks on fatigue fracture surface of steel 1

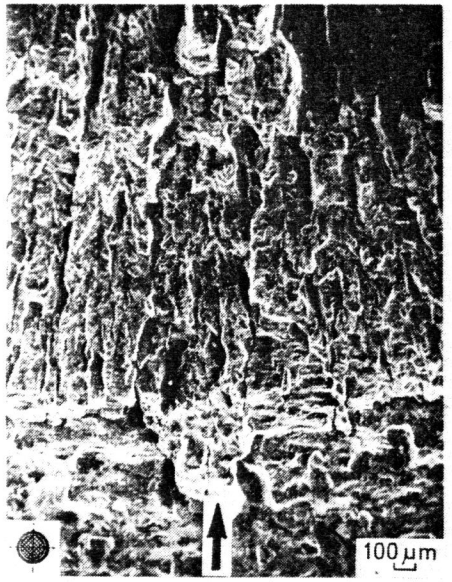

Fig.8 Fatigue fracture surface of steel 2 with "blocky"structure (0,12 % carbon)

Fig.9 Cracks ahead of the main crack front (arrows)

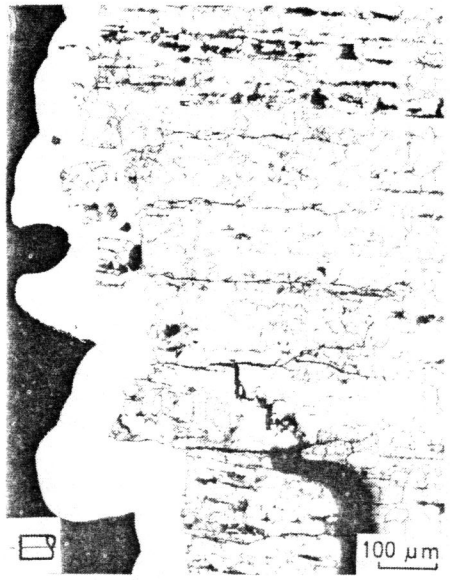

Fig.10 Longitudinal micro-section (Ni-plated) of the fatigued specimen in low carbon steel 2

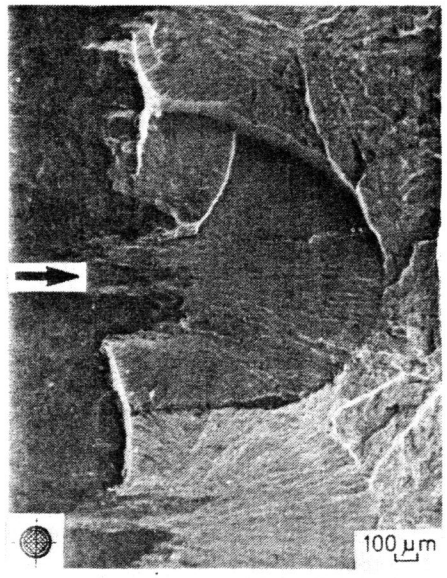

Fig.11 "Factory roof" fracture surface in quenched and tempered steel 3